

Comparison of ablatators for the polar direct drive exploding pusher platform

Heather D. Whitley^{a,1}, G. Elijah Kemp^a, Charles Yeamans^a, Zachary Walters^a, Brent E. Blue^a, Warren Garbett^b, Marilyn Schneider^a, R. Stephen Craxton^c, Emma M. Garcia^c, Patrick W. McKenty^c, Maria Gatu-Johnson^d, Kyle Caspersen^a, John I. Castor^a, Markus Däne^a, C. Leland Ellison^a, James Gaffney^a, Frank R. Graziani^a, John Klepeis^a, Natalie Kostinski^a, Andrea Kritcher^a, Brandon Lahmann^d, Amy E. Lazicki^a, Hai P. Le^a, Richard A. London^a, Brian Maddox^a, Michelle Marshall^a, Madison E. Martin^a, Burkhard Militzer^e, Abbas Nikroo^a, Joseph Nilsen^a, Tadashi Ogitsu^a, John Pask^a, Jesse E. Pino^a, Michael Rubery^b, Ronnie Shepherd^a, Philip A. Sterne^a, Damian C. Swift^a, Lin Yang^a, Shuai Zhang^c

^a*Lawrence Livermore National Laboratory, Livermore, California 94550, USA*

^b*AWE plc, Aldermaston, Reading RG7 4PR, United Kingdom*

^c*Laboratory for Laser Energetics, University of Rochester, Rochester, New York 14623, USA*

^d*Massachusetts Institute of Technology, Plasma Science and Fusion Center, Cambridge, Massachusetts 02139, USA*

^e*University of California, Berkeley, California 94720, USA*

Abstract

We examine the performance of pure boron, boron carbide, high density carbon, and boron nitride ablatators in the polar direct drive exploding pusher (PDXP) platform. The platform uses the polar direct drive configuration at the National Ignition Facility to drive high ion temperatures in a room temperature capsule and has potential applications for plasma physics studies and as a neutron source. The higher tensile strength of these materials compared to plastic enables a thinner ablator to support higher gas pressures, which could help optimize its performance for plasma physics experiments, while ablatators containing boron enable the possibility of collecting additional data to constrain models of the platform. Applying recently developed and experimentally validated equa-

*Manuscript prepared for the proceedings of IFSA2019.

Email address: whitley3@llnl.gov (Heather D. Whitley)

¹Presenting and corresponding author

tion of state models for the boron materials, we examine the performance of these materials as ablators in 2D simulations, with particular focus on changes to the ablator and gas areal density, as well as the predicted symmetry of the inherently 2D implosion.

Keywords: direct drive, exploding pusher, ablators, inertial confinement fusion

1. Introduction

The Polar Direct Drive Exploding Pusher (PDXP) platform was proposed and developed as a platform for studying electron-ion temperature equilibration and thermal conduction in the high energy density regime that is relevant to inertial confinement fusion at the National Ignition Facility (NIF)[1, 2, 3] It has since been applied in both nucleosynthesis experiments[4] and as a neutron source.[5, 6] Our initial PDXP proposal for NIF called for a thin ablator, enabling full ablation of the capsule shell, which we believed would lead to better uniformity of the plasma during the proposed time-resolved spectroscopic measurements of the plasma temperature. Early design studies indicated that the performance for heat flow measurements was optimized with a gas fill pressure of 8-10 atm based on 500 kJ of laser energy incident on a 3 mm outer diameter capsule. Because the proposed measurements of plasma temperature rely on using Ar as a spectroscopic dopant, the platform required that the signal from the Ar spectral lines must be significantly higher than the emission from the background plasma, and the Ar mass in the target must be well known. We had initially considered SiO₂ or Be ablators for these measurements due to the ability to fabricate thin capsules of either material. The SiO₂ design was ruled out due to calculations that showed high background emission, and thus low Ar signal, during the proposed measurement, and Be was ruled out because the sputtering process used to make Be ablators generally results in significant Ar remaining in the shell. For these reasons, and the lack of capabilities to build high density carbon (HDC) capsules of the desired size at the time, we based our point design on glow discharge polymer (GDP) ablators, which necessitated

capsules of $\sim 20 \mu\text{m}$ thickness for the desired fill pressure.[7] The initial shots were thus fielded using 3 mm diameter GDP capsules with thicknesses of 18-20 μm and $\sim 8 \text{ atm}$ gas fill. The inflight implosion self-emission measurements and post-shot simulations from these initial shots (N160920-003, N160920-005, N160921-001, N170212-003, and N170212-004) indicated slight inflight asymmetry early in the implosion and a very asymmetric shell at bang time.[1, 4, 8]

The laser pulse design in PDXP was motivated by the general concepts associated with the design of exploding pushers; the optimal design results from a rapid, impulsive ablation of the capsule, driving very high ion temperatures in the fill gas.[9] The optimization of the pulse for the initial design of the heat flow platform was completed by examining a series of 1D radiation hydrodynamic simulations and choosing a pulse that optimized the window of time available for electron and ion temperature measurements. This resulted in a 1.8 ns square pulse and computed ablator mass remaining of about 30% at the end of the pulse. All subsequent shots on this platform have similarly used pulse shapes where the majority of the laser energy is delivered during a square pulse, and 1D simulations of those shots indicate a similar amount of remaining mass, based on the total mass contained within the contour of electron density corresponding to the critical surface for laser absorption at 351 nm wavelength ($\sim 9 \times 10^{21} \text{ cm}^{-3}$), regardless of laser drive or capsule geometry. Although these capsules are driven by relatively short laser pulses, 2D simulations show that the laser beams tend to continually imprint a specific pattern on the imploding shell, and this imprint appears to contribute to the observed capsule asymmetry at bang time based on comparison of the self-emission images from N170212-003 and N170212-004 to 2D simulations.[4]

One possible route for mitigating the asymmetry, which would presumably allow for the generation of more uniform plasma conditions, would be to design capsules that have a thinner ablator with better coupling to the laser. Such an ablator could potentially enable the use of a shorter pulse, and the higher thermal conductivity of a higher density material could help to mitigate the non-uniformity of the laser energy deposition. Due to the linear relation between

tensile strength and capsule burst pressure,[7] materials such as boron (B), high density carbon (HDC), boron carbide (B_4C), and boron nitride (BN), which have tensile strength 5-10 times higher than that of GDP, could presumably support the 8-10 atm fill pressures of the nominal PDXP point design at substantially reduced thickness relative to GDP. While HDC is now a common capsule material, our interest in boron-containing materials is motivated by the possibility of collecting data to help constrain simulation models of the PDXP platform. In PDXP capsules with a DT gas fill, high yields can be achieved, and thus comparing gamma reaction history (GRH) measurements[10, 11] from implosions using an ablator containing natural boron to measurements using a GDP capsule could potentially provide constraining data for the gas areal density during burn due to the impact of knock-on deuterons on the $^{11}B(d,n\gamma_{15.1})^{12}C$ reaction on the GRH.[12] In addition, our best fitting simulations of previous shots invoke a diffusive mix model for ablator-fuel mix.[1] The $^{10}B(\alpha,p\gamma)^{13}C$ reaction, which produces γ signals around 3.5 MeV, could provide data to help distinguish between diffusive mix and hydrodynamic instabilities, potentially validating the use of this diffusive mix model.[13] We note that our interest in the pure B and BN ablators is specifically motivated by the absence of carbon in these ablators, which eliminates potential cross talk from other reactions with C.[14] These same reactions with C are useful for constraining shell areal density based on GRH data[15], but would complicate the diagnostics we propose here for examining the gas density and distinguishing between diffusive mix and hydrodynamic instabilities.

Over the past several years, advances in additive manufacturing and target fabrication techniques have made the possibility of fielding shots with B_4C ablators more tangible.[16] Novel techniques have also been applied to make targets for planar equation of state experiments on BN at the NIF.[17] It therefore seems timely to examine these materials as potential ablators. We are not currently aware of a fabrication technique for making a pure B capsule, though we include our results for B for future comparison purposes. We present a brief summary of simulations examining the performance of B, B_4C , HDC, and BN ablators

in 2D. Our 2D models are based on previously developed post-shot models for N160920-005, which fielded a GDP ablator and 8 atm D_2 gas fill at room temperature. Due to the inherent uncertainties in modeling capsule implosions, we seek to minimize controllable sources of error in this work. As a prelude to this study, we therefore applied a variety of theoretical methods to examine the equation of state (EOS) of pure boron, B_4C , and BN[18, 19, 20] since these materials have not yet been used in capsule experiments at the NIF. New EOS models were developed for B and BN based on our earlier work, and we make use of a previously developed and recently tested model for B_4C [20, 21] in this baseline comparison study. The EOS of HDC and GDP were also previously studied in detail.[21, 22, 23]

2. Model description and results

Our 2D direct drive simulations are carried out using the Ares radiation hydrodynamics simulation code.[24, 25] For the purpose of this study, we use N160920-005 as the baseline for tuning the initial model and we use the laser pulse as delivered in this shot for all simulations reported here. In this shot, we fielded a 2.955 mm outer diameter GDP with a 19 μm thickness ablator, filled with 7.941 atm of D_2 gas with 5×10^{-4} atomic fraction of Ar as a spectroscopic dopant. The capsule was driven with a 1.8 ns square pulse, delivering 479 kJ of total energy with slightly higher power in the outer beams to provide additional power near the equator of the capsule.[1] The calculated power profile on the capsule surface is shown in Figure 1. We use a laser ray trace method for depositing the energy in the capsule, which takes into account the 3D pointing geometry, but does not include the effects of cross-beam energy transfer or nonlocal electron thermal transport. Both of these effects are known to be important for modeling laser-matter interactions in direct drive implosions,[26, 27, 28, 29] but we have nonetheless found that the salient features of our shots are modeled well using a more approximate treatment. Our models employ multi-group diffusion for the propagation of radiation, and we apply a flux

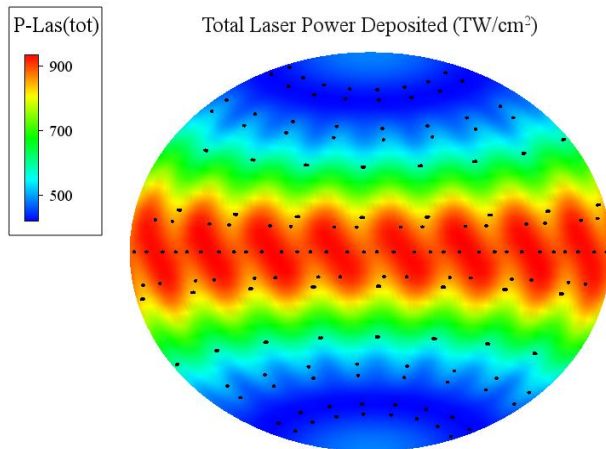


Figure 1: Computed laser power on the capsule surface for N160920-005. The black dots indicate the pointing on the capsule surface.

limiter to the electron thermal conduction in the ablator during the laser pulse. We tune the flux limiter and a multiplier on the total laser power to fit the observed x-ray bang time of the shot, as described in Ref. [1]. In this study, we used a flux limiter of 0.0398, and we find a good fit to the neutron bang time by assuming an energy multiplier of 0.875. We have also applied the multicomponent Navier-Stokes (mcNS) model for species diffusion in simulations of this shot, and we find that using this model enables a good match to the measured burn-averaged ion temperature and the neutron yield, provided that a multiplier is applied to the diffusion coefficient.[1] However, we have no reason to expect that the multiplier that we determined for the GDP capsules will also apply to the ablators considered in this study, and so we did not exercise the species diffusion model in this study.

Table 1 summarizes the ablator characteristics of the 2D simulations performed in this study. For HDC, we considered both a thin design and a thicker design. For the thicker design, the ablator thickness was chosen to be $6.0 \mu\text{m}$

Ablator	Thickness (μm)	Capsule Mass (mg)	Density (g/cc)	EOS Models
GDP	19	0.54	1.046	L5400[21, 22]
HDC	6	0.54	3.32	L9061[23]
B	6	0.40	2.46	L52[18]
B ₄ C	5.86	0.40	2.52	L2122[21, 20]
BN	6	0.37	2.25	L2152[19] and L2150
HDC	4.45	0.40	3.32	L9061[23]

Table 1: Capsule parameters and EOS models used in this study.

in order provide a mass match to the GDP ablator, whereas for the thinner designs, we first considered an HDC capsule where the total ablator mass is reduced to 0.4 mg, corresponding to a thickness of 4.45 μm . The thicknesses of the B and B₄C ablators were then chosen to match the total mass of the thinner HDC design (6.0 μm and 5.86 μm , respectively). Similar to HDC, BN can exist either in a cubic (diamond) lattice or in a hexagonal (graphitic) lattice. In this work, we consider BN in the hexagonal phase, with a density of 2.25 g/cc, so the mass of the BN ablator is just slightly lower than that of the other thin capsule designs. The BN capsule was chosen to have a thickness that matches the thin HDC capsule.

Table 1 also lists the equation of state model used for each material in the table. For BN, we applied both a model that was recently developed (L2152)[19] and an older model from the LEOS library that was developed by D. A. Young and is based on a Thomas-Fermi model (L2150). These two models were compared in our previous report on the BN equation of state.[19] For each of these calculations, we assumed a D₂ fill pressure of 7.941 atm at room temperature, which was chosen to match N160920-005. We use the L1014 model for the EOS of D₂, consistent with our previous 1D simulation studies.[1, 18, 20]

Table 2 lists some of the computed results for each of the capsules. The

Ablator/thickness (μm)	Absorbed Energy (kJ)	Neutron Yield	Convergence Ratio	T_{ion} (keV)
GDP/19	282	4.4×10^{13}	9.8	7.2
HDC/6	324	9.1×10^{13}	10	8.8
B/6	310	6.2×10^{13}	5	15
B ₄ C/5.86	313	6.5×10^{13}	5	15
BN/6	319	6.7×10^{13}	5	16
HDC/4.45	324	7.8×10^{13}	5	15

Table 2: Results from 2D Ares simulations. The convergence ratio is computed based on the minimum gas volume. We note that the measured neutron yield from N160920-005 was $2.11(\pm 0.1) \times 10^{13}$, so the clean yield computed in the 2D calculation of the GDP capsule is about a factor of 2 larger than the experiment.

total yield of the capsules predictably increases as a function of the total energy absorbed. Since the laser-capsule coupling is higher for the higher density ablators, the HDC and BN ablators produce the highest neutron yields. We also find that the two HDC capsules absorb the same amount of energy from the laser, but the thicker ablator produces higher yield, higher peak convergence ratio (CR) defined based on the ratio of the initial gas volume to the minimum gas volume, $CR = (V_i/V_{min})^{1/3}$, and lower burn-averaged ion temperature. The performance of the thicker HDC capsule appears to mimic that of the thick GDP capsule. Results for the BN capsule are reported only for L2152 because the results from L2150 were nearly identical. As expected, the thin capsule with low ablator density near peak compression is not sensitive to the choice of EOS model. (For the thicker capsules, variations in the EOS can impact the computed performance, and we explore EOS variations in greater depth in Ref. [20].)

In Figures 2-4 we plot several characteristic properties of the gas from simulations of the thicker GDP and HDC capsules (Figures 2 and 3), as well as the

thinner B_4C capsule (Figure 4) as a function of time. In each of these plots, the burn rate is scaled by its peak value and the average ion temperature in the gas is scaled by the burn-averaged ion temperature listed in Table 2. We also plot the average radius of the gas scaled by the initial radius, which is equivalent to the convergence ratio as defined above and listed in Table 2. These plots demonstrate that the two thick capsule designs behave similarly, with most of the neutrons being produced after the peak in the average gas temperature, while the gas is still being compressed by the remaining ablator. In contrast, the thin capsule design produces its yield at the same time as the ion temperature peaks. The average ion temperature in the thin capsule design also exceeds the burn-averaged ion temperature, in contrast to the thick capsule designs. In the thick designs, the burn is occurring primarily after shock convergence. This is consistent with what we found in our 1D study, as shown in Figures 2 and 7 of Ref. [1], though in 2D the shock structure is more complicated and the burn is diminished mostly due to capsule break up, as opposed to capsule expansion, near peak compression. The break up of the capsule occurs due to lower density regions that are generated at the points where the inner laser beams impact the capsule.

Comparing Figures 2 and 3 provides some insight into why the HDC capsule produced a factor of 2 higher neutron yield than the GDP capsule. First, the increase in absorbed laser power for HDC relative to GDP leads to a stronger shock, and hence higher ion temperatures. Second, the higher density ablator provides more remaining mass during stagnation, hence the capsule break up that leads to the demise of burn in the GDP calculation is less severe for HDC. Third, the HDC implosion is slightly more symmetric than the GDP implosion. The better symmetry and decreased breakup are evident in the scaled radius vs. time plot for HDC (Fig 3), which shows a more obvious minimum at peak compression than the GDP capsule.

Analogous to the similarity in the HDC and GDP thick capsules, we find that all of the thin capsule designs behave in a similar fashion, regardless of the identity of the ablator, producing similar yield, extremely high burn-averaged

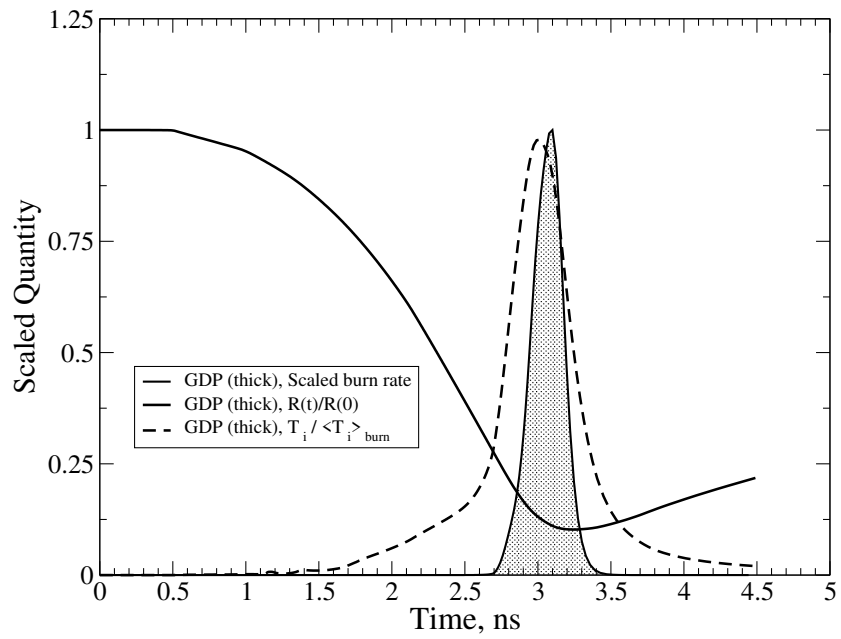


Figure 2: Scaled burn rate (shaded curve), average radius (solid), and average ion temperature (dashed) as a function of time for the GDP design, as described in the text. The burn in the thicker GDP design takes place primarily after the peak average temperature in the gas is reached, implying that compression of the gas is contributing to the overall yield.

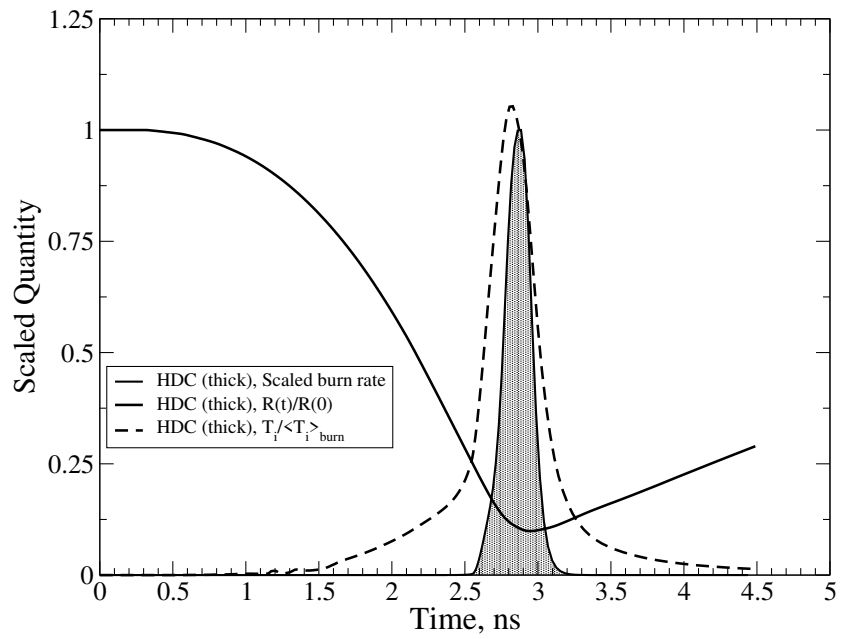


Figure 3: Scaled burn rate (shaded curve), average radius (solid), and average ion temperature (dashed) as a function of time for the thicker HDC design, as described in the text. Similar to the GDP capsule, the burn in the thicker HDC design takes place following the peak in average ion temperature.

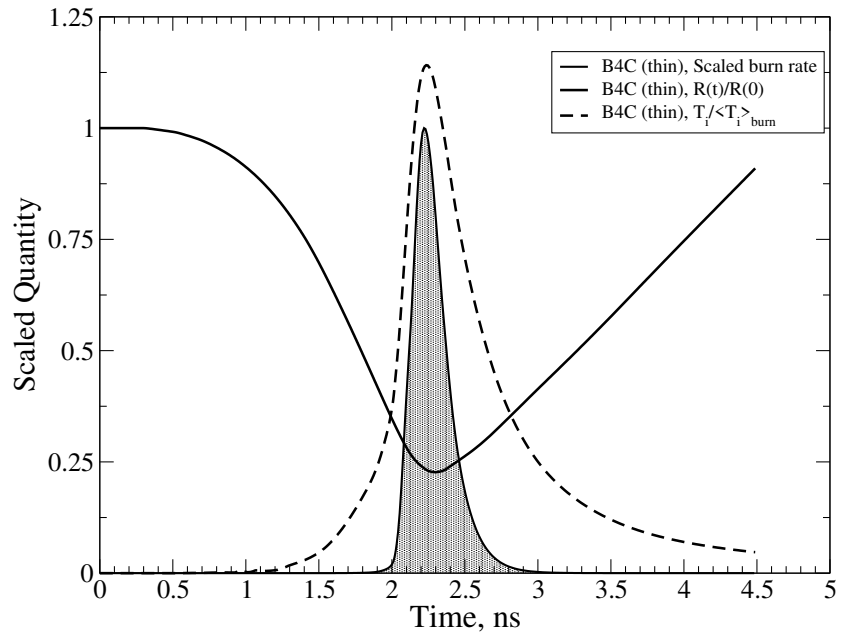


Figure 4: Scaled burn rate (shaded curve), average radius (solid), and average ion temperature (dashed) as a function of time for the thinner B₄C design, as described in the text. In contrast to the thicker HDC and GDP designs, the burn takes place primarily during the peak in the average gas ion temperature. The compression in the thinner capsule design is also lower than it is for either the HDC or GDP thick capsules.

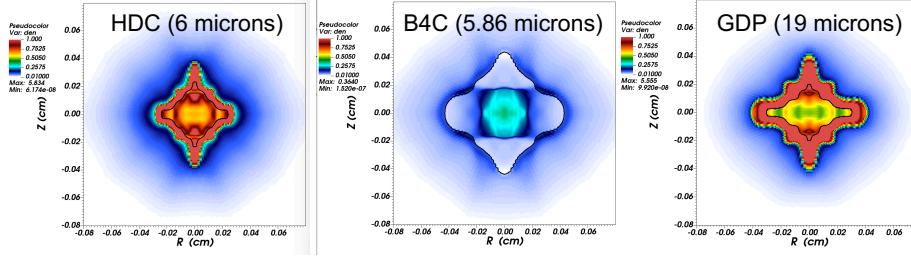


Figure 5: Computed density profiles near peak compression for the HDC (left) and GDP (right) thicker capsule designs. The thinner B₄C (center) design shows significantly lower overall density than the other two capsules. The color map is the same in all three images. For the thinner B₄C design, the peak density of 0.36 g/cc occurs within the center of the gas and is surrounded by a region of lower density gas that extends out to about 400 μm in each direction. The thicker ablators exhibit peak densities of > 5.5 g/cc, and the peak density occurs in the remaining ablator that surrounds the gas.

ion temperatures (15-16 keV) and about a factor of 2 lower convergence ratio than the thicker capsule designs. Figure 5 shows the density profile at peak compression for the B₄C thinner capsule design along with the computed density near peak compression for both the HDC and GDP thicker capsules. The black contour in each plot is the boundary between the ablator and the gas. In the thinner capsules, the ablator has burned away, and the overall gas density is consequently lower than it is for the thicker capsules, consistent with the lower convergence shown in Fig. 4. As discussed above, Figure 5 also shows that the HDC capsule produces a more uniform compression of the gas than the GDP ablator. All of the computed geometries at peak stagnation show significant asymmetry due to the polar direct drive configuration. This indicates that the proposed heat flow experiments would still require significant design advances in order to realize a more uniform plasma, even with the use of a thinner ablator.

3. Summary and Conclusions

In this paper we have presented a survey of candidate ablator materials for future experiments on the PDXP platform. Our simulations show that thinner capsule designs using the higher tensile strength materials should lead to more complete ablation of the capsule than the baseline GDP design. However, our calculations also show that, even in the case where a thinner ablator is used, the polar direct drive configuration is still predicted to imprint significant asymmetry on the implosion that persists through stagnation. Due to the inherent uncertainties in modeling direct drive implosions and the lack of experimental data to validate our models for ablators other than GDP, we have not yet pursued additional optimization of either the laser pointing or the laser pulse in this study. It is possible that using a thinner ablator composed of any one of these materials and re-optimizing the drive for the new geometry would lead to a more symmetric implosion. Ideally, such optimization of the laser pulse would be performed using a baseline model that had been fit to experimental data for the actual ablator under consideration. As such, we have saved this study as future work, and we hope that this work provides motivation for future experiments on this platform.

Even with the apparent lack of symmetry, the increased coupling of the laser to the higher density materials improves the neutron yield in these implosions. One interesting finding of this study is that an HDC version of N160920-005 is predicted to give about a factor of 2 higher neutron yield than the GDP ablator. While the HDC capsule does give a slightly more symmetric geometry and somewhat higher gas density, the higher yield is primarily the result of better laser-target coupling, which produces a stronger shock and higher ion temperatures than the GDP capsule. Because the increase in yield can be largely attributed to better laser-capsule coupling, moving to an HDC capsule on the PDXP platform for neutron source development[5] appears to be a low risk change that would give higher yields than those that could be achieved in the current GDP-based experiments.

While we have observed that the 2D model gives a reasonable fit to some of the diagnostic data obtained for N160920-005, modeling these direct drive simulations at the NIF is still relatively uncertain. In the PDXP platform in particular, it is not clear what fraction of the yield is produced due to the strong shock versus what fraction comes from the compression of the gas by ablator material that remains after the laser pulse. These calculations demonstrate large differences in the ablator areal density during the burn of the gas. Ablators containing natural boron could enable us to determine whether the computed ablator areal density is realistic based on GRH measurements. Demonstrating the feasibility of those studies will require more detailed analysis of these simulations to determine whether there would be a measurable effect of remaining ablator mass on the GRH measurement.

Acknowledgments. This research was in part based upon work supported by the Department of Energy National Nuclear Security Administration under Award Number DE-NA0003856. Part of the work was performed under the auspices of the U.S. Department of Energy by Lawrence Livermore National Laboratory under Contract No. DE-AC52-07NA27344. H. D. Whitley acknowledges the support of the PECASE award. Contributions from the AWE are under the UK Ministry of Defence © Crown Owned Copyright 2020/AWE.

This document was prepared as an account of work sponsored by an agency of the United States government. Neither the United States government nor any agency thereof, nor any of their employees, makes any warranty, express or implied, or assumes any legal liability or responsibility for the accuracy, completeness, or usefulness of any information, apparatus, product, or process disclosed, or represents that its use would not infringe privately owned rights. Reference herein to any specific commercial product, process, or service by trade name, trademark, manufacturer, or otherwise does not necessarily constitute or imply its endorsement, recommendation, or favoring by the U.S. Government or any agency thereof. The views and opinions of authors expressed herein do not necessarily state or reflect those of the U.S. Government or any agency thereof,

and shall not be used for advertising or product endorsement purposes.

References

- [1] C. L. Ellison, H. D. Whitley, C. R. D. Brown, S. R. Copeland, W. J. Garbett, H. P. Le, M. B. Schneider, Z. B. Walters, H. Chen, J. I. Castor, R. S. Craxton, M. Gatu Johnson, E. M. Garcia, F. R. Graziani, G. E. Kemp, C. M. Krauland, P. W. McKenty, B. Lahmann, J. E. Pino, M. S. Rubery, H. A. Scott, R. Shepherd, H. Sio, Development and modeling of a polar direct-drive exploding pusher platform at the National Ignition Facility, *Physics of Plasmas* 25 (7) (2018) 072710. doi:10.1063/1.5025724.
- [2] A. R. Miles, H.-K. Chung, R. Heeter, W. Hsing, J. A. Koch, H.-S. Park, H. F. Robey, H. A. Scott, R. Tommasini, J. Frenje, C. K. Li, R. Petrasso, V. Glebov, R. W. Lee, Numerical simulation of thin-shell direct drive DHe3-filled capsules fielded at OMEGA, *Physics of Plasmas* 19 (7) (2012) 072702. doi:10.1063/1.4737052.
- [3] S. Skupsky, J. A. Marozas, R. S. Craxton, R. Betti, T. J. B. Collins, J. A. Delettrez, V. N. Goncharov, P. W. McKenty, P. B. Radha, T. R. Boehly, J. P. Knauer, F. J. Marshall, D. R. Harding, J. D. Kilkenny, D. D. Meyerhofer, T. C. Sangster, R. L. McCrory, Polar direct drive on the national ignition facility, *Physics of Plasmas* 11 (5) (2004) 2763–2770. doi:10.1063/1.1689665.
- [4] M. Gatu Johnson, D. T. Casey, M. Hohenberger, A. B. Zylstra, A. Bacher, C. R. Brune, R. M. Bionta, R. S. Craxton, C. L. Ellison, M. Farrell, J. A. Frenje, W. Garbett, E. M. Garcia, G. P. Grim, E. Hartouni, R. Hatarik, H. W. Herrmann, M. Hohensee, D. M. Holunga, M. Hoppe, M. Jackson, N. Kabadi, S. F. Khan, J. D. Kilkenny, T. R. Kohut, B. Lahmann, H. P. Le, C. K. Li, L. Masse, P. W. McKenty, D. P. McNabb, A. Nikroo, T. G. Parham, C. E. Parker, R. D. Petrasso, J. Pino, B. Remington, N. G. Rice, H. G. Rinderknecht, M. J. Rosenberg, J. Sanchez, D. B. Sayre, M. E.

- Schoff, C. M. Shulberg, F. H. Séguin, H. Sio, Z. B. Walters, H. D. Whitley, Optimization of a high-yield, low-areal-density fusion product source at the National Ignition Facility with applications in nucleosynthesis experiments, *Physics of Plasmas* 25 (5) (2018) 056303. doi:10.1063/1.5017746.
- [5] C. B. Yeamans and B. E. Blue, National Ignition Facility neutron sources, Technical Report No. LLNL-CONF-739397, Lawrence Livermore National Laboratory, 2018. [link].
URL <https://www.osti.gov/servlets/purl/1458648>
- [6] C. Yeamans, G. E. Kemp, Z. B. Walters, P. W. McKenty, E. M. Garcia, Y. Yang, R. S. Craxton, B. E. Blue, High yield polar direct drive fusion neutron sources at the National Ignition Facility, *Submitted to Nuclear Fusion*.
- [7] A. Nikroo, D. G. Czechowicz, K. C. Chen, M. Dicken, C. Morris, R. Andrews, A. Greenwood, E. Castillo, Mechanical properties of thin GDP shells used as cryogenic direct drive targets at OMEGA, *Fusion Science and Technology* 45 (2) (2004) 229–232. doi:10.13182/FST45-2-229.
- [8] The shots in September 2016 were designed to provide calibration data for the 2D simulations and examine whether symmetry could be improved via modifications in the cone fraction. As such, we tested three different cone fractions (0.33, 0.28, and 0.22, respectively for N160920-003, N160920-005, and N160921-003.) We chose to use N160920-005 for this study because it showed the best in-flight symmetry. More complete results from these shots will be included in a future report.
- [9] M. D. Rosen, J. H. Nuckolls, Exploding pusher performance: A theoretical model, *The Physics of Fluids* 22 (7) (1979) 1393–1396. doi:10.1063/1.862752.
- [10] H. Geppert-Kleinrath, Y. Kim, K. D. Meaney, H. W. Herrmann, N. M. Hoffman, J. A. Carrera, A. L. Kritcher, M. S. Rubery, A. Leatherland,

High bandwidth DT reaction history measurements in inertial confinement fusion, *Bulletin of the American Physical Society* Vol. 64.

- [11] D. B. Sayre, L. A. Bernstein, J. A. Church, H. W. Herrmann, W. Stoeffl, Multi-shot analysis of the gamma reaction history diagnostic, *Review of Scientific Instruments* 83 (10) (2012) 10D905. doi:10.1063/1.4729492.
- [12] A. C. Hayes-Sterbenz, G. M. Hale, G. Jungman, and M. W. Paris, Probing the Physics of Burning DT Capsules Using Gamma-ray Diagnostics, Technical Report No. LA-UR-15-20627, Los Alamos National Laboratory, 2015. doi:10.2172/1169150.
- [13] A. C. Hayes, Applications of nuclear physics, *Reports on Progress in Physics* 80 (2) (2017) 026301. doi:10.1088/1361-6633/80/2/026301.
- [14] Anna Sterbenz-Hayes, private communication.
- [15] K. D. Meaney, Y. H. Kim, H. W. Herrmann, H. Geppert-Kleinrath, N. M. Hoffman, Improved inertial confinement fusion gamma reaction history 12c gamma-ray signal by direct subtraction, *Review of Scientific Instruments* 90 (11) (2019) 113503. doi:10.1063/1.5092501.
- [16] R. Chen, Q. Shi, L. Su, M. Yang, Z. Huang, Y. Shi, Q. Zhang, Z. Liao, T. Lu, Preparation of a b4c hollow microsphere through gel-casting for an inertial confinement fusion (ICF) target, *Ceramics International* 43 (1, Part A) (2017) 571 – 577. doi:10.1016/j.ceramint.2016.09.196.
- [17] W. D. Frane, O. Cervantes, G. Ellsworth, J. Kuntz, Consolidation of cubic and hexagonal boron nitride composites, *Diamond and Related Materials* 62 (2016) 30 – 41. doi:10.1016/j.diamond.2015.12.003.
- [18] S. Zhang, B. Militzer, M. C. Gregor, K. Caspersen, L. H. Yang, J. Gaffney, T. Ogitsu, D. Swift, A. Lazicki, D. Erskine, R. A. London, P. M. Celliers, J. Nilsen, P. A. Sterne, H. D. Whitley, Theoretical and experimental investigation of the equation of state of boron plasmas, *Phys. Rev. E* 98 (2018) 023205. doi:10.1103/PhysRevE.98.023205.

- [19] S. Zhang, A. Lazicki, B. Militzer, L. H. Yang, K. Caspersen, J. A. Gaffney, M. W. Däne, J. E. Pask, W. R. Johnson, A. Sharma, P. Suryanarayana, D. D. Johnson, A. V. Smirnov, P. A. Sterne, D. Erskine, R. A. London, F. Coppari, D. Swift, J. Nilsen, A. J. Nelson, H. D. Whitley, Equation of state of boron nitride combining computation, modeling, and experiment, *Physical Review B* 99 (16) (2019) 165103. doi:10.1103/PhysRevB.99.165103.
- [20] S. Zhang, M. C. Marshall, L. H. Yang, P. A. Sterne, B. Militzer, M. Däne, J. A. Gaffney, A. Shamp, T. Ogitsu, K. Caspersen, A. E. Lazicki, D. Erskine, R. A. London, P. M. Celliers, J. Nilsen, H. D. Whitley, Benchmarking boron carbide equation of state using computation and experiment, *Phys. Rev. E* 102 (2020) 053203. doi:10.1103/PhysRevE.102.053203.
- [21] P. A. Sterne, L. X. Benedict, S. Hamel, A. A. Correa, J. L. Milovich, M. M. Marinak, P. M. Celliers, D. E. Fratanduono, Equations of state for ablator materials in inertial confinement fusion simulations, *Journal of Physics: Conference Series* 717 (2016) 012082. doi:10.1088/1742-6596/717/1/012082.
- [22] S. Zhang, B. Militzer, L. X. Benedict, F. Soubiran, P. A. Sterne, K. P. Driver, Path integral Monte Carlo simulations of dense carbon-hydrogen plasmas, *J. Chem. Phys.* 148 (10) (2018) 102318. doi:10.1063/1.5001208.
- [23] L. X. Benedict, K. P. Driver, S. Hamel, B. Militzer, T. Qi, A. A. Correa, A. Saul, E. Schwegler, Multiphase equation of state for carbon addressing high pressures and temperatures, *Phys. Rev. B* 89 (2014) 224109. doi:10.1103/PhysRevB.89.224109.
- [24] R. M. Darlington, T. L. McAbee, G. Rodrigue, A study of ALE simulations of rayleigh-taylor instability, *Computer Physics Communications* 135 (1) (2001) 58 – 73. doi:10.1016/S0010-4655(00)00216-2.
- [25] B. E. Morgan, J. A. Greenough, Large-eddy and unsteady RANS simula-

tions of a shock-accelerated heavy gas cylinder, *Shock Waves* 26 (4) (2016) 355–383. doi:10.1007/s00193-015-0566-3.

- [26] N. S. Krasheninnikova, J. A. Cobble, T. J. Murphy, I. L. Tregillis, P. A. Bradley, P. Hakel, S. C. Hsu, G. A. Kyrala, K. A. Obrey, M. J. Schmitt, et al., Designing symmetric polar direct drive implosions on the Omega Laser Facility, *Physics of Plasmas* 21 (4) (2014) 042703. doi:10.1063/1.4870756.
- [27] T. J. Murphy, N. S. Krasheninnikova, G. Kyrala, P. A. Bradley, J. A. Baumgaertel, J. Cobble, P. Hakel, S. C. Hsu, J. L. Kline, D. Montgomery, et al., Laser irradiance scaling in polar direct drive implosions on the National Ignition Facility, *Physics of Plasmas* 22 (9) (2015) 092707. doi:10.1063/1.4931092.
- [28] P. Radha, M. Hohenberger, D. Edgell, J. Marozas, F. Marshall, D. Michel, M. Rosenberg, W. Seka, A. Shvydky, T. Boehly, et al., Direct drive: Simulations and results from the National Ignition Facility, *Physics of Plasmas* 23 (5) (2016) 056305. doi:10.1063/1.4946023.
- [29] A. B. Zylstra, C. Yeamans, S. Le Pape, A. MacKinnon, M. Hohenberger, D. N. Fittinghoff, H. Herrmann, Y. Kim, P. B. Radha, P. W. McKenty, R. S. Craxton, M. Hoppe, Enhanced direct-drive implosion performance on nif with wavelength separation, *Physics of Plasmas* 27 (12) (2020) 124501. doi:10.1063/5.0021015.